

---

**Polycarboxylate-based superplasticizer with added silica sub-microspheres for use in Portland cement materials**

**Superplastificante a base de policarboxilato con adición de sub-microesferas de sílice para uso en materiales de cemento Portland**

M.J. Ungsson-Nieblas<sup>1</sup>, E. Rubio-Rosas<sup>2</sup>, R.A. Vargas-Ortíz<sup>1</sup>, A. Bórquez-Mendivil<sup>1</sup>, F.G. Cabrera-Covarrubias<sup>1</sup>, A. Castro-Beltrán<sup>1</sup>, B.A. García-Grajeda<sup>1</sup>, J.L. Almaral-Sánchez<sup>1\*</sup>

<sup>1</sup>Universidad Autónoma de Sinaloa, Fuente de Poseidón y Prol. Ángel Flores S/N., Los Mochis, Sinaloa, 81223, México.

<sup>2</sup>Benemérita Universidad Autónoma de Puebla, Centro Universitario de Vinculación y Transferencia de Tecnología, Prol. 24 sur S/N CU San Manuel Puebla, Pue. C.P. 72570, México.

Received: May 28, 2023; Accepted: August 7, 2023

---

**Abstract**

A new polycarboxylate, PCE, based superplasticizer was synthesized with added silica sub-microspheres, Ss (Ss-PCE), from the synthesis of these two components, for use in Portland-cement materials. PCE was synthesized from the copolymerization of methacrylic-acid and poly(ethylene-glycol)-methacrylate. Ss ( $\approx 200$  nm) were synthesized from Stöber-method. Ss-PCE was obtained with the addition of Ss (5% by weight-PCE). Four cement pastes and mortars were prepared. The characteristic bonds of PCE, Ss and Ss-PCE were identified (FT-IR), the average size (HRTEM) and structure (XRD) of Ss were defined. The hydration products of cement pastes (3, 7 and 28 curing days) were identified (XRD). The compressive strength of the mortars was obtained (ASTM-C109/C109M-20). The success of our work was to synthesize PCE and Ss to form Ss-PCE, and to improve the performance of cementitious materials modified with them, this offers the possibility of continuing this research later because both PCE and Ss were synthesized, and it will be possible to delve into its behavior. In addition, was defined that the initial hydration process of  $C_3S$  in Portland cement slowed down significantly and the compressive strength of the modified mortars was increased (3, 7 and 28 days) due to Ss-PCE.

**Keywords:** Portland cement, silica sub-microspheres, polycarboxylates, hydration products.

---

**Resumen**

Se sintetizó un nuevo superplastificante basado en policarboxilato, PCE, con sub-microesferas de sílice añadidas, Ss (Ss-PCE), a partir de la síntesis de estos dos componentes, para su uso en materiales de cemento-Portland. El PCE se sintetizó por copolimerización de ácido-metacrílico y poli(etilenglicol)-metacrilato. Ss ( $\approx 200$  nm) se sintetizaron por el método de Stöber. Ss-PCE se obtuvo por adición de Ss (5% peso-PCE). Se prepararon cuatro pastas y morteros de cemento. Se identificaron los enlaces característicos de PCE, Ss y Ss-PCE (FT-IR), se definió el tamaño promedio (HRTEM) y la estructura (XRD) de Ss. Se identificaron los productos de hidratación de las pastas de cemento (3, 7 y 28 días-curado) (XRD). Se obtuvo la resistencia a compresión de morteros (ASTM-C109/C109M-20). El éxito de nuestro trabajo fue sintetizar PCE y Ss para formar Ss-PCE y mejorar el comportamiento de los materiales cementicios modificados con ellos, esto ofrece la posibilidad de continuar esta investigación más adelante porque se sintetizaron PCE y Ss, y se podrá profundizar en su comportamiento. Además, se definió que el proceso inicial de hidratación del  $C_3S$  en cemento Portland se ralentizó significativamente e incrementó la resistencia a compresión de los morteros modificados (3, 7 y 28 días) debido al Ss-PCE.

**Palabras clave:** Cemento Portland, sub-microesferas de sílice, policarboxilatos, productos de hidratación, superplastificante.

---

\*Corresponding author. E-mail: [jalmaral@uas.edu.mx](mailto:jalmaral@uas.edu.mx)

<https://doi.org/10.24275/rmiq/Proc2348>

ISSN:1665-2738, issn-e: 2395-8472

## 1 Introduction

Silica particles can be synthesized from alkoxide precursor sources, including tetraethyl orthosilicate (TEOS), by different mechanisms such as sol-gel and Stöber method (Castruita-de León *et al.*, 2018; Reyna-Martínez *et al.*, 2020; Huynh *et al.*, 2020). The silica nanoparticles added to the cement-based materials have influence in the following aspects: a) the compressive strength is increased, due to the fact that they reacted with the  $\text{Ca}(\text{OH})_2$ , also known as portlandite (P), to form additional hydrated calcium silicate (CSH) gel, (Najigivi *et al.*, 2013; Yu *et al.*, 2020) b) hydration and setting time are reduced (Lavergne *et al.*, 2019; Singh *et al.*, 2013) because improve resistance to water permeability (Ardalan *et al.*, 2017), c) the modified concrete durability is enhanced since the cohesion of the interfacial transition zone (cement paste-aggregate) is increased because the nanopores present in them can be filled with the silica nanoparticles (Zhuang & Chen, 2019) and d) improve the microstructure of the cement paste by granting greater homogeneity, density, and compaction (Haruehansapong *et al.*, 2014), in addition to providing a more stable and stronger bonding (Shih *et al.*, 2006). The mortar and concrete, with nanosilica (nS) dosages of 1.5% to 2.0% by weight and coarser nanoparticles (264 nm) provide enhanced in mechanical and durability properties compared to the finer nanoparticles (36 nm). (Puerto Suárez *et al.*, 2022). In other works, nS dosages of 0.5-2% by weight, enhanced in 25% the mechanical properties in cement concrete, and dosages of 4% enhanced the compressive strength at 28 days (Raheem *et al.*, 2021). Cement mortar compressive strength increased by the use of microsilica (2.8%) and nanosilica (9%) contents, by weight, as replacement of cement content (Kooshkaki & Eskandari-Naddaf, 2019).

A superplasticizer is structured by high molecular weight long chain anionic surfactants with numerous polar groups in its hydrocarbon chain, which significantly reduces the surface tension of water around concrete making it more fluid. The use of superplasticizer in mixing concrete can reduce the amount of water mixture by 20-30%, compared to the 5-10% reduction achieved with common plasticizer admixtures, maintaining its high consistency (Kumar Mehta & Monteiro, 2006). Superplasticizers are classified into four major types, according to their chemical composition: a) sulfonated melamine-formaldehyde (SMF), b) sulfonated naphthalene-formaldehyde condensates (SNF), c) modified lignosulfonates (MLS), and d) polycarboxylate ether derivatives (PCE) (Zhu *et al.*, 2022).

The PCE are composed of two main elements: a) the carboxylate group, which is anionic and

allows interaction with the cement surface to produce dispersion and b) a polyethylene oxide side chain or a mixture of polyethylene-polypropylene to increase dispersion (Lei *et al.*, 2022). PCE eliminates the segregation of concrete, gives it excellent dispersion of cement particles in water and accelerates the rate of hydration, setting and hardening (Khudhair *et al.*, 2018), therefore, it increases the compressive strength and workability of concrete (Pereira *et al.*, 2012), which increases the surface potential force, the solid-liquid affinity, and the steric hindrance (Sathyan *et al.*, 2018; Tian *et al.*, 2019), and prolongs the initial and final setting times (Zhao *et al.*, 2018). PCE superplasticizers were used to modify the surface of the sand in the preparation of the cement mortar and increased its compressive strength at 7 and 28 days of age (Noaman *et al.*, 2020). Cement pastes treated with polycarboxylate synthesized with ester-based had better behaviour of dispersibility, fluidity retention and viscosity than those treated with polycarboxylate with amide-based (Lin *et al.*, 2021). PCE copolymers based on isoprenyl ether, vinyl, allyl, and methacrylate macromonomers were synthesized and it was found that those with higher hydrophilic-lipophilic balance (HLB) values significantly reduced the plastic viscosity of mortars and concretes and low water-to-cement ratios. PCEs based on allyl ether-maleic acid showed very high HLB values, while methacrylate-ester and PCE vinyl ether were very low (Lange & Plank, 2015). A low sensitivity PCE (P-DMG) was synthesized from the copolymerization of esterified macromonomers with hydroxyethyl acrylate, acrylic acid, 4-hydroxybutyl vinyl polyoxyethylene ether, and acryloyloxyethyl trimethyl ammonium chloride, and the P-DMG showed better performance than the conventional polycarboxylates, because it reduced the water/cement ratio, the temperature and its workability (Guan *et al.*, 2020). A PCE with longer polyoxyethylene side chains was synthesized and less retarding influence on cement hydration and rapid early strength development of hardened concrete were achieved (Xia *et al.*, 2020). A polyamidoamine dendrimer-based polycarboxylic superplasticizer (DPC) with a crosslinked emanative structure was synthesized by simple free radical polymerization. Its addition to the cement paste produced a delay in the heat of hydration, reducing it at an early age (3 and 7 days) and with a substantial increase in its compressive strength than blank cement samples (Zhao *et al.*, 2018).

The nS were modified with PCE under microwave irradiation conditions and the PCE was grafted on the nS surface, they were compared with unmodified nS, both in the saturated solution of calcium hydroxide, and it turned out that the modified nS had better dispersion, stability, also better compatibility with PCE, with improved fluidity of the fresh cement

paste (Huang & Wang, 2017). nS colloidal amorphous particles dispersed in commercial PC (GnS) 15% solids (with particles ranges between 3 and 150 nm) was used in quaternary cement formulations comprising Portland cement (PC), limestone powder (LS) and fly ash (FA) (Papatzani & Paine, 2018).

In an exhaustive review of the literature, we only found one work about the synthesis and properties of nS-doped polycarboxylate superplasticizer, however, nS is commercial reagent with mean particle size of 12 nm and PCE was synthesized from other precursors different from our work, and the cement hydration process was not analyzed (Ren *et al.*, 2020). The success of our work was to synthesize the two components, PCE and Ss (average size 200 nm) to form Ss-PCE, and improve its properties for use in cementitious materials, which offers the opportunity to continue this research subsequently, improve their composition (because both, Pc and Ss are synthesized) and optimize the properties of the Ss-PCE. Ss were characterized by XRD and HRTEM. Ss, PCE and Ss-PCE were analyzed by FT-IR. Hydration process of cement pastes was analyzed by XRD, and compressive strength of the mortar was obtained at 3, 7 and 28 days. In this work, a superplasticizer was synthesized from the coupling of 200 nm mean size silica sub-microspheres (Ss) with PCE, both synthesized and added to mixing water to make cement-based materials. Ss were characterized by XRD and HRTEM. Ss, PCE, and Ss-PCE were analyzed by FT-IR. Hydration process of cement pastes was analyzed by XRD, and compressive strength of the mortar was obtained at 3, 7, and 28 days.

## 2 Material and methods

### 2.1 Materials

The superplasticizer additive was elaborated from synthesis of Ss and PCE. For synthesis of Ss were necessary: tetraethylorthosilicate (TEOS,  $\text{Si}(\text{OC}_2\text{H}_5)_4$ ), CAS No. 78-10-4 (reagent grade, 98%), as  $\text{SiO}_2$  source, ammonium hydroxide ( $\text{NH}_4\text{OH}$ ), CAS No. 1336-21-6 (ACS reagent, 28.0-30.0%  $\text{NH}_3$  basis), as catalyst, deionized water ( $\text{H}_2\text{O}$ ), CAS No. 7732-18-5, and pure ethyl alcohol ( $\text{CH}_3\text{CH}_2\text{OH}$ ), CAS No. 64-17-5 (200 proof, anhydrous,  $\geq 99.5\%$ ) as solvents. For the synthesis of PCE, the following reagents were used: poly(ethylene glycol)-methacrylate (PEG-MA,  $\text{H}_2\text{C}=\text{C}(\text{CH}_3)\text{CO}_2(\text{CH}_2\text{CH}_2\text{O})_n\text{CH}_3$ ), CAS No. 25736-86-1 (average Mn 500, contains 900 ppm monomethyl ether hydroquinone as inhibitor), to form the main

chain, sodium persulfate (SPS,  $\text{Na}_2\text{S}_2\text{O}_8$ ), CAS No. 7775-27-1 (reagent grade,  $\geq 98\%$ ), as initiator, methacrylic acid (MAA,  $\text{H}_2\text{C}=\text{C}(\text{CH}_3)\text{COOH}$ ), CAS No. 79-41-4 (contains 250 ppm MEHQ as inhibitor, 99%), and 2-methyl-2-propene-1-sulfonic acid sodium salt (MPSA,  $\text{H}_2\text{C}=\text{C}(\text{CH}_3)\text{CH}_2\text{SO}_3\text{Na}$ ), CAS No. 1561-92-8 (98%), as catalysts and deionized water as solvent. All reagents are from the Sigma-Aldrich brand and were purchased from the Merck company. For the manufacture of the mortar specimens, natural sand extracted from the river and type III ordinary Portland cement established by ASTM C150 (CPC) CEMEX brand were purchased from the local company, Materiales y Agregados Guasave, S.A. de C.V., and potable water were used.

### 2.2 Synthesis of silica sub-microspheres (Ss)

The Ss were synthesized by the Stöber method at room temperature (Huynh *et al.*, 2020; Mohammadpour *et al.*, 2019; Stöber *et al.*, 1968) from 23.43 ml of TEOS, 40 ml of EtOH, 55 ml of  $\text{H}_2\text{O}$ , and 20 ml of  $\text{NH}_4\text{OH}$ . The synthesis began with the hydrolysis of TEOS in a mixture of EtOH,  $\text{H}_2\text{O}$ , and  $\text{NH}_4\text{OH}$  (catalyst), which stabilized the reaction, by generating electrostatic repulsion due to ammonia ions ( $\text{NH}_4^+$ ), to convert the methoxy groups ( $\text{SiOCH}_3$ ) in silanol ( $\text{SiOH}$ ), then, this solution was stirred for 1 h, until condensed and a gel was obtained, which was washed in alcohol to remove chemical residues, filtered for 24 h, then centrifuged to separate the solids from the solvent to obtain powders (Ss). In Figure 1 is shown the obtaining powders (Ss) by the Stöber method.

### 2.3 Synthesis of the polycarboxylate (PCE) and superplasticizer (Ss-PCE)

The synthesis of PCE and Ss-PCE. PCE was synthesized by free radical copolymerization of MAA and PEG-MA, following procedures described before (Plank *et al.*, 2008, 2009). 100 ml of deionized water, 12.9 ml of MAA, and 50 ml of PEG-MA were added in a Vessel-type reactor; this solution was stirred for 5 minutes, then, 3 gr of MPSA (dissolved in 15 ml of deionized water) was added and stirring continued for 15 minutes. Subsequently, the pH was set to 9 and an aqueous solution of 1.5 g of SPS, as initiator, in 15 ml of deionized water was added, to start the polymerization, which was carried out at 80 °C for 1 h. The reaction mixture was then allowed to cool down to room temperature. Ss-PCE was synthesized from a mixture of PCE and Ss. This mixture was formed by adding 5 % by weight of Ss to the PCE, then stirred for 15 minutes at room temperature (Figure 2).

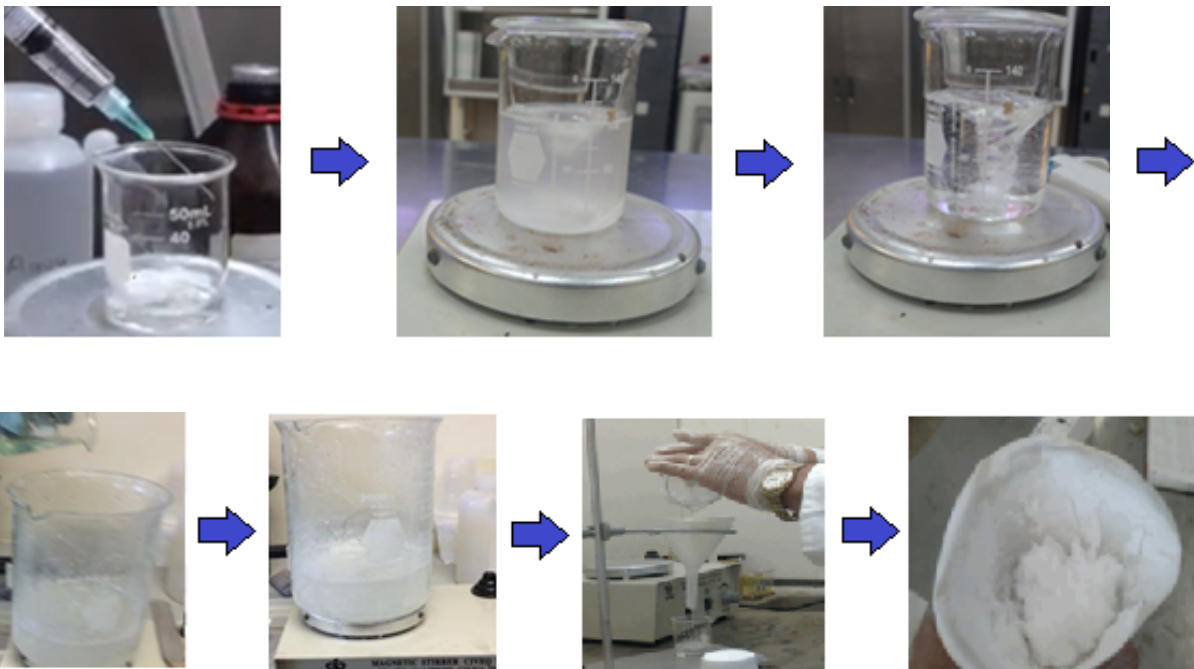


Figure 1. Obtaining powders (Ss) by the Stöber method.

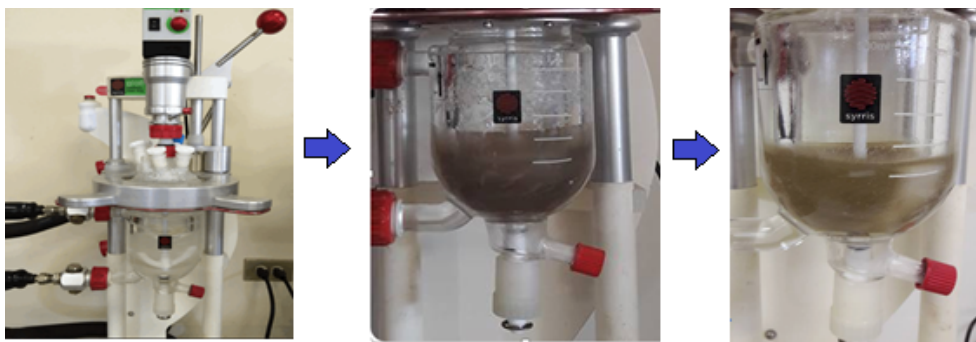


Figure 2. Synthesis of PCE and Ss-PCE.

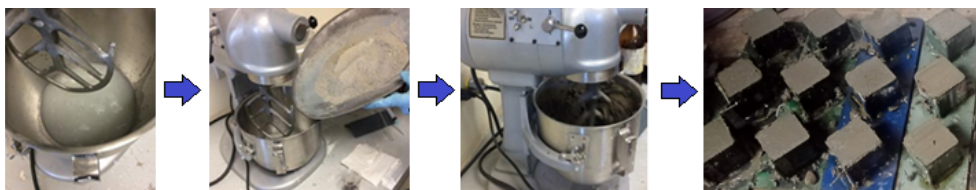


Figure 3. Elaboration of cement pastes modified with PCE, Ss and Ss-PCE.

#### 2.4 Cement paste mixes and mortar mixes

Four cement pastes mixes were prepared according with ASTM C305-20: 1) Cement paste without additives (CP), 2) Cement paste with the addition of Ss (SsP), 3) Cement paste with the addition of PCE

(PCEP), and 4) Cement paste with addition of Ss-PCE (Ss-PCEP). The mixing water was modified for SsP, PCEP, and Ss-PCEP, with the addition of correspond dosage of Ss, PCE, and Ss-PCE, respectively, and stirred by 30 minutes (Figure 3). Table 1 shows the dosages of the compounds for each paste mixture type.

Table 1. The dosages of the compounds for each paste mixture type.

Sample	w/c	Ss (%wt, Portland cement)	PCE (%wt, Portland cement)	Ss-PCE (%wt, Portland cement)
CP	0.4	-	-	-
SsP	0.4	1	-	-
PCEP	0.4	-	1	-
Ss-PCEP	0.4	-	-	1



Figure 4. Elaboration of cement mortars modified with PCE, Ss and Ss-PCE.

Table 2. The dosages of the mixtures for 1 m<sup>3</sup> of mortar.

Sample	w/c	Cement Portland (kg)	Fine aggregate (kg)	Ss (% wt. cement Portland)	PCE (% wt. cement Portland)	Ss-PCE (% wt. cement Portland)
RM	0.4	1333	3667	0	0	0
SsM	0.4	1333	3667	1	0	0
PCEM	0.4	1333	3667	0	1	0
Ss-PCEM	0.4	1333	3667	0	0	1

Four types of mortar mixtures were designed according with ASTM C<sub>305</sub>-20. A reference mortar, RM and three modified mortars with PCE (PCEM), Ss (SsM) and Ss-PCE (Ss-PCEM) at cured age of 3, 7 and 28 days were made. The addition of the superplasticizer was carried out under the same procedure as in the preparation of the cement pastes (Figure 4).

Table 2 shows the dosages of the mixtures for 1 m<sup>3</sup> of mortar, for RM, SsM, PCEM, and Ss-PCEM. Ratio w/c, and amounts of cement Portland (kg) and fine aggregate (kg) are constants, while the amount of Ss, PCE, and Ss-PCE is 1% wt. cement Portland for SsM, PCEM, and Ss-PCEM, respectively.

## 2.5 Characterizations

The microstructural, size and morphology of Ss were analyzed by high-resolution transmission electron microscopy (HRTEM) in a JEOL JEM-2200FS+Cs equipped with a spherical aberration corrector in the condenser lens and operated at an accelerating voltage of 200 kV.

The main bonds of Ss, PCE, and Ss-PCE were characterized by Fourier transform infrared spectroscopy (FT-IR), using an Infrared spectrometer, Bruker brand model Vertex70. For the analysis, the samples were pulverized in an agate mortar and deposited on the diamond surface of the attenuated total reflectance (ATR) system, the analysis was performed in the wavelength range between 4000-400 cm<sup>-1</sup>, the instrument has a fixed spectral resolution of 4 cm<sup>-1</sup>.

The composition phase of Ss and cement pastes were identified for the powder X-ray diffraction (XRD) technique. The analysis was carried out in a Bruker D8 Discover brand diffractometer. The samples were pulverized in an agate mortar and placed in a sample holder, the powder was compressed to compact. X-rays with a wavelength = 1.5406 Å,

operated at 35 kV and 25 mA, were used, the crystalline phases were identified using the 2013 PDF4 + database of the International Center for Diffraction Data (ICDD).

The compressive strength was evaluated for the mortar samples, according to ASTM C109/C109M-20 (ASTM-International, 2021), using INSTRON 600DXR2081 universal testing machine at a crosshead speed of 1 mm/min with a span ratio of 16:1. Three 5X5X5 cm cubic mortar specimens for each age (3,7, and 28 days) were made, then covered with a plastic film to prevent moisture loss and after 24 hrs they were removed from the mold and cured in immersion until they were tested.

## 3 Results and discussion

### 3.1 Ss size (High-resolution transmission electron microscope, HRTEM)

Figure 5 shows a HRTEM micrograph of the silica obtained by the Stöber method, this confirms the synthesis of monodisperse and spherical particles with an average diameter of 200 nm. This average was obtained with the measure of 210 nanoparticles, which showed homogeneous size distribution and uniformly dispersed in the area and diameters in the range of 194 to 209 nm.

### 3.2 Ss structure (X-ray diffraction)

Figure 6 shows the XRD pattern corresponding to the Ss obtained by the Stöber method. The diffractogram shows a broad band with a maximum peak at 2θ = 23°, that confirms that the Ss are composed of non-crystalline silica.

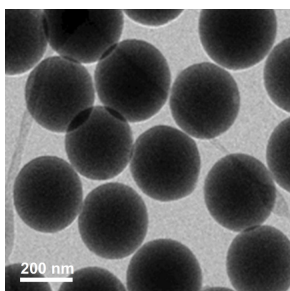


Figure 5. HRTEM micrograph of the silica obtained by the Stöber method, where monodisperse and spherical particles with a mean diameter of 200 nm are observed.

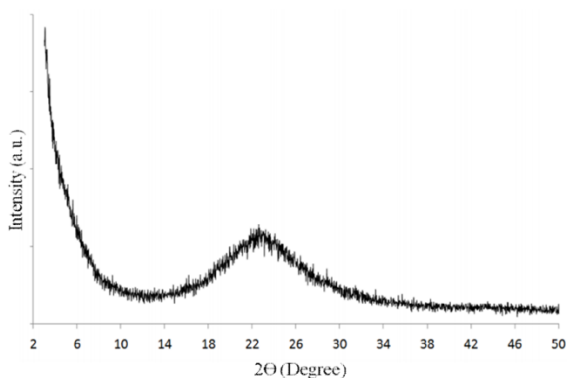


Figure 6. X-ray diffraction pattern of Ss.

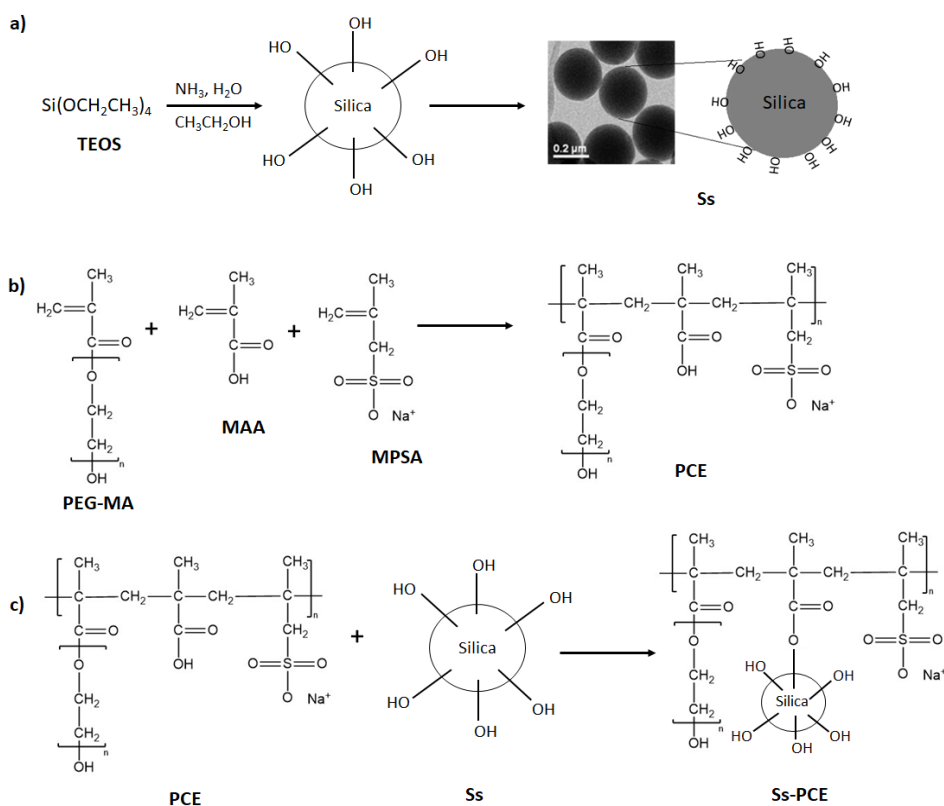


Figure 7. Scheme of proposed reaction mechanism of Ss, PCE and Ss-PCE.

### 3.3 Proposed Reaction Mechanism of Ss, PCE and Ss-PCE

Figure 7 shows a scheme of proposed reaction mechanism. In a) Ss formation with OH groups by the Stöber method is shown. In b), PCE formation by free radical copolymerization of PEG-MA and MAA is indicated, using MPSA as catalyst. In c), Ss-PCE formation from a mixture of PCE and Ss, which the Ss are coated with the carboxylate, through OH groups on the surface of the Ss. Then, if an alkaline medium is present, it enables the condensation of the PCE with the Ss, achieving anchorage through Si-O- covalent bonds (Ren *et al.*, 2020).

### 3.4 Ss, PCE, and Ss-PCE characteristics bonds (Fourier transform infrared spectroscopy, FT-IR)

Figure 8 shows the FT-IR spectra of: a) Ss, b) PCE, and c) Ss-PCE. In a), the band at  $3420 \text{ cm}^{-1}$  is attributed to OH bonding in stretch-type vibration mode in Si-structures. The bands observed at  $1080 \text{ cm}^{-1}$  and  $800 \text{ cm}^{-1}$  are associated to the stretching asymmetric vibration of Si-O-Si bonds and the band at  $950 \text{ cm}^{-1}$  can be attributed to Si-OH stretching (Vlasenkova *et al.*, 2019). In b), the broad band observed at  $3435\text{-}3410 \text{ cm}^{-1}$  is attributed to stretching O-H bonds due to hydrogen bond formation (Lv *et al.*,

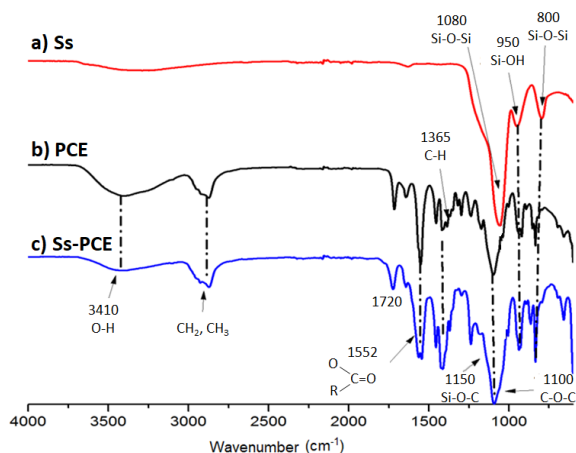


Figure 8. The FT-IR spectra of: a) Ss, b) PCE, and c) Ss-PCE.

2012; Ma, 2010), the bands shown at 2921-2869  $\text{cm}^{-1}$  are associated with  $\text{CH}_2$ ,  $\text{CH}_3$  bonds, present in the methyl/methylene group of the chain. In the interval 1728-1716  $\text{cm}^{-1}$  appears a band corresponding to  $\text{COO}^-$  and in 1647-1634  $\text{cm}^{-1}$  attributed to the  $-\text{OH}$  bonds present in  $\text{H}_2\text{O}$ . The 1570-1549  $\text{cm}^{-1}$  band is a characteristic of the asymmetric strain of  $\text{COO}^-$ , part of a carboxylic group of a metal salt. The bands from 1116  $\text{cm}^{-1}$  to 1102  $\text{cm}^{-1}$  are attributed to ether-binding characteristics to C-O-C asymmetric strain vibration of aliphatic ethers (Chen, 2013; Ghorab *et al.*, 2012; Habbaba *et al.*, 2013). The bands observed between 955-947  $\text{cm}^{-1}$  are associated with the type of  $\text{CH}_3$  bending vibration, of the methyl functional group adjacent to a carbon atom, and at 849-835  $\text{cm}^{-1}$  to the bending of  $\text{CH}_3$ , the methyl group adjacent to an oxygen atom. In c), the characteristic bands corresponding to Ss (950 and 800  $\text{cm}^{-1}$ ) and PCE (3435-3410  $\text{cm}^{-1}$ , 2921-2869  $\text{cm}^{-1}$ , 1728-1716  $\text{cm}^{-1}$ , 1647-1634  $\text{cm}^{-1}$ , 1570-1549  $\text{cm}^{-1}$ , 1116-1102  $\text{cm}^{-1}$ , 955-947  $\text{cm}^{-1}$  and 849-835  $\text{cm}^{-1}$ ), which shows that Ss-PCE is formed, because were founded characteristic bands of both compose, Ss and PCE. In addition, a shoulder was identified at 1150  $\text{cm}^{-1}$ , this is attributed to the presence of the Si-O-C bond (A.S. Zakirov *et al.*, 2007; J. Essmeister *et al.*, 2023) which indicates the condensation between the OH groups present on both, Ss surface and PCE (Figure 7), this confirms the successful formation of Ss-PCE.

### 3.5 Hydration process of modified cement pastes (X-ray diffraction)

Figure 9 show the XRD patterns of four series of samples, CP, SsP, PCEP, and Ss-PCEP, for curing ages of 3, 7 and 28 days. In CP and SsP, the intensity of the peaks of the crystalline phase that corresponds to  $\text{Ca}(\text{OH})_2$ , calcium hydroxide (Portlandite, P), increases with the curing time, which is attributed to continuous hydration of the  $\text{C}_2\text{S}$ , dicalcium silicate

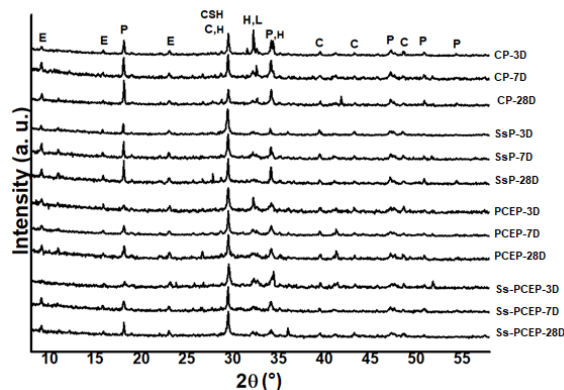


Figure 9. The X-ray diffraction patterns of the four series of samples, CP, SsP, PCEP, and Ss-PCEP.

(Larnite, L), and  $\text{C}_3\text{S}$ , tricalcium silicate phases (Hatrurite, H). Furthermore, it is also possible to detect the characteristic XRD peaks of non-hydrated calcium silicates (L, H) and it is observed that the intensity decreases with the curing time. Meanwhile, the intensity of the peak that characterizes the CSH superimposed on that of  $\text{CaCO}_3$ , calcium carbonate (Calcite, C) increases with the age of hydration, this change is also related to the progress of hydration for 28 days (Madadi & Wei, 2022). The peaks that characterize to  $\text{CaCO}_3$  (C) could also be detected in the diffraction patterns and overlap with those CSHs. Finally, even when the percentage of Ss added to the sample (SsP) is low, a lower intensity of the  $\text{C}_2\text{S}$  (L) phase is observed. In this sense, a pozzolanic reaction by the presence of the Ss was detected (Zhao *et al.*, 2017).

In PCEP and Ss-PCEP, is confirmed the formation of the CSH and  $\text{Ca}(\text{OH})_2$  (P) phases as the main hydration products. The peaks that characterize the anhydrous cement clinker  $\text{C}_2\text{S}$  (L) and  $\text{CaCO}_3$  (C) can also be clearly observed in the XRD patterns. It can be observed that the intensities of the diffraction peaks, which characterize  $\text{C}_3\text{S}$  (H) and  $\text{C}_2\text{S}$  (L) decrease with the curing time. It can be clearly seen that the characteristic peaks of  $\text{Ca}(\text{OH})_2$  (P) have a lower intensity of the XRD peaks, which is correlated with the presence of PCE in Portland cement, and that delays the evolution of this crystalline phase. The retarding effect on the hydration process is in agreement with the previous literature (Ren *et al.*, 2014).

### 3.6 Compressive strength of mortars (ASTM C109/C109M-20)

Figure 10 shows the compressive strength of RM, PCEM, SsM, and Ss-PCEM at cured age of 3, 7 and 28 days. The results of PCEM show that PCE did not influence in the compressive strength of cement mortar at 3 days of cured, compared with RM. This could be because the PCE present higher

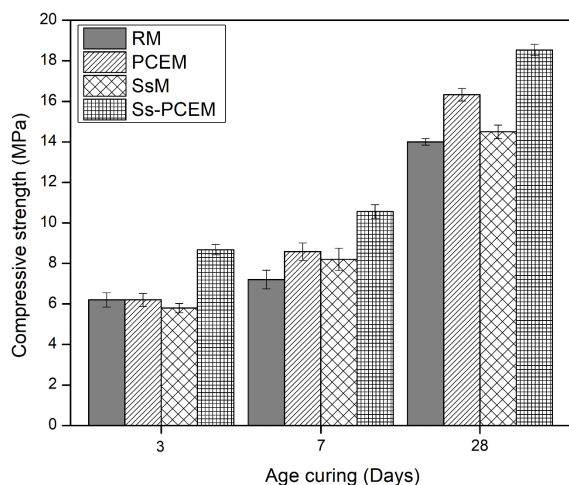


Figure 10. Compressive strength of mortars: reference (RM) and modified (PCEM, SsM and Ss-PCEM).

adsorption capacity and could be adsorbed through their functional groups in the cement (superficial layer of its particles) and this process hinders its early hydration and slows it (Ren *et al.*, 2020). However, this property increased 19.2 and 16.7 %, respectively, at 7 and 28 days. This behavior can be attributed to the fact that the polycarboxylate, due to their comb structure, were adsorbed on the surface of the cement particles and its side chains extended to the liquid phase, which produced a steric repulsion between the cement and thus generates an electrostatic repulsion to produce the glue breakdown. During this interaction, an aqueous film composed of the dissolving agent is formed on the surface of the cement particles, which, in addition to presenting some mechanical resistance, also has the characteristic of lubricating the spaces between the particles and the aggregates of the cement mixture. In addition, the structure of the mortar become more compact because the cement has a flocular structure that promotes the hydration of its grout, which positively influences a uniform dispersion. The carboxylate group present in the polycarboxylate may have the ability to easily form a complex with the hydrated  $\text{Ca}^{2+}$  present in the cement, this increases the bond strength between cementitious materials and allows reducing the amount of mixing water needed, shrinkage in capillary and internal pore size, this translates into more compact microcracks that improve the resistance of the mortar (J. Chen *et al.*, 2022). The compressive strength of SsM decreased slightly in 6.5 % at 3 days of cured, compared with RM, however, increased 13.9 and 3.6%, at 7 and 28 days, respectively. This enhancing can be attributed to pozzolanic reaction during the cement hydration process. Also, the Ss would have the ability of fill the pores present in the cement matrix (Haruehansapong *et al.*, 2014; Jo *et al.*, 2007). The compressive strength of Ss-PCEM increased, compared to RM, in 40, 46.7 and 32.35 %, for all curing ages studied, 3, 7, and

28 days, respectively. These results can be explained by the particular behavior of PCEs and Ss, detailed above. For the PCEs, by substantially improving the dispersion of the cement particles in the Ss-PCEM, they could have increased their compactness. On the other hand, the Ss would favor a high polymerization of the C-S-H gels, in addition, they could be released from the Ss-PCE when the cement hydrates, producing the additional pozzolanic reaction with the CH. The previous contributions of PCE and Ss, together, increased the compressive strength of the Ss-PCEM at 28 days (Papatzani & Paine, 2018; Ren *et al.*, 2020).

## Conclusions

Polycarboxylate-based superplasticizer with added silica sub-microspheres for use in Portland cement materials was synthesized successfully, according to follow:

The Ss were synthesized by the Stöber method, which was verified by observing their average size of 200 nm (HRTEM) and amorphous structure (XRD).

A proposal for reaction mechanism were established about Ss formation with OH groups by the Stöber method is shown, PCE formation by free radical copolymerization of PEG-MA and MAA, using MPSA as catalyst, and Ss-PCE formation from a mixture of PCE and Ss, which the Ss are linked with the PCE through OH groups of both.

The synthesis of PCE, Ss and Ss-PCE was verified by identifying their characteristic bonds (FT-IR),  $\text{CH}_2$ ,  $\text{CH}_3$ , C-O-C and  $\text{COO}^-$  for PCE, Si-O-Si and Si-OH for Ss, and the presence of bonds of both components for Ss-PCE, moreover, a shoulder was identified at  $1150 \text{ cm}^{-1}$ , this is attributed to the presence of the Si-O-C bond.

The slowing down of hydration at early ages of cement in reference cement paste and modified with PCE, Ss and Ss-PCE, was demonstrated by the identification of their hydration products (E, P, CSH, C, H and L), at curing ages of 3, 7 and 28 days (XRD), due to  $\text{Ca}(\text{OH})_2$  increased with the curing time, which attributed to continuous hydration of the  $\text{C}_2\text{S}$  and  $\text{C}_3\text{S}$ .

The compressive strength of mortar add with Ss-PCE increased, compared to reference mortar, for each curing age (3, 7, and 28 days). due to the contribution of its components (PCEs and Ss): the PCEs, by substantially improving the dispersion of the cement particles in the Ss-PCEM, and Ss would favor a high polymerization of the C-S-H gels when the cement hydrates, producing the additional pozzolanic reaction with the CH.



## Acknowledgment

This work was financially supported by the DGIP of the Universidad Autónoma de Sinaloa (UAS), through the PROFAPI2014/010 Project, by the Consejo Nacional de Ciencia y Tecnología (CONACYT) through the CB/2014/241622 Project, and for its contribution of Scholarship No. 261575. We thank the Benemérita Universidad Autónoma de Puebla for its support in infrastructure and equipment. We kindly thank Prof. Rosalba Fuentes Ramírez of Universidad de Guanajuato for her assistance in interpreting measurements.

## Nomenclature

C <sub>2</sub> S	Dicalcium silicate
C <sub>3</sub> S	Tricalcium silicate
CaCO <sub>3</sub>	Calcite, C
Ca(OH) <sub>2</sub>	Portlandite, calcium hydroxide
CP	Cement paste without additives
CSH	Hydrated calcium silicate
DPC	Polyamidoamine dendrimer-based polycarboxylic superplasticizer
FA	Fly ash
FT-IR	Fourier Transform Infrared Spectroscopy
GnS	Commercial colloidal amorphous polycarboxylate dispersed nS particles
H - C <sub>3</sub> S	Hatruite phase
HLB	Hydrophilic-lipophilic balance
HRTEM	high-resolution transmission electron microscopy
L - C <sub>2</sub> S	Larnite, L
LS	Limestone powder
MAA	Methacrylic acid
MLS	Modified lignosulfonates
MPSA	2-methyl-2-propene-1-sulfonic acid sodium salt
nS	Nanosilica
NS/PCE	Nanosilica/polycarboxylate ether derivatives
P	Portlandite, calcium hydroxide
PCE	Polycarboxylate
PC	Portland cement
PCE	Polycarboxylate ether derivatives
PCEM	Mortar modified with PCE
PCEP	Cement paste with the addition of PCE
P-DMG	Low sensitivity polycarboxylate superplasticizer
PEG-MA	poly(ethylene-glycol)-methacrylate
RM	Reference mortar
SMF	Sulfonated melamine-formaldehyde
SNF	Sulfonated naphthalene-formaldehyde condensates
SsM	Mortar modified with Ss

SsP	Cement paste with the addition of Ss
Ss-PCE	Superplasticizers
Ss-PCEM	Mortar modified with Ss-PCE
Ss-PCEP	Cement paste with addition of Ss-PCE
Ss	Silica sub-microspheres
TEOS	Tetraethylorthosilicate
XRD	X-ray diffraction

## References

- Ardalan, R. B., Jamshidi, N., Arabameri, H., Joshaghani, A., Mehrinejad, M., & Sharafi, P. (2017). Enhancing the permeability and abrasion resistance of concrete using colloidal nano-SiO<sub>2</sub> oxide and spraying nanosilicon practices. *Construction and Building Materials* 146, 128-135. <https://doi.org/10.1016/j.conbuildmat.2017.04.078>
- ASTM-International. (2021). ASTM C 39/C 39M - 21. Standard Test Method for Compressive Strength of Cylindrical Concrete Specimens. 3-9. <https://doi.org/10.1520/C0039-C0039M-21>
- Castruita-de León, G., Meléndez-Ortiz, H.I., Perera-Mercado Y.A., Mercado-Silva, J.A., García-Cerda, L.A., Montes-Luna, A. de J., & García-Rodríguez, S.P. (2018). Effect of silica source on the synthesis and properties of polysulfone/silica composite membranes for gas separation. *Revista Mexicana de Ingeniería Química* 17(2), 693-705. <https://doi.org/10.24275/10.24275/uam/izt/dcbi/revmexingquim/2018v17n2/Castruita>
- Chen, B. (2013). Synthesis of a macromer, MPEGAA, used to prepare an AMPS-modified polyacrylic acid superplasticizer. *Journal of Wuhan University of Technology-Mater. Sci. Ed.* 28(6), 1186-1190. <https://doi.org/10.1007/s11595-013-0842-y>
- Chen, J., Zhu, Y., Du, W., Li, M., Wang, Y., Zhang, C., Shi, M., & Xue, B. (2022). Influence of polycarboxylate superplasticizer on the properties of cement-fly ash cementitious materials and concrete. *Sustainability (Switzerland)* 14(20). <https://doi.org/10.3390/su142013440>
- Essmeister, J., Schachtner, L., Szoldatits, E., Schwarz, S., Lichtenegger, A., Baumann, B., Föttinger, K. & Konegger, T. (2023). Polymer-derived Ni/SiOC materials structured by vat-based photopolymerization with catalytic activity in CO<sub>2</sub> methanation. *Open Ceramics*

- 14, 100350. <https://doi.org/10.1016/j.oceram.2023.100350>
- Ghorab, H. Y., Kenawi, I. M., & Abdel All, Z. G. (2012). Interacción entre cementos de diferente composición y aditivos superplastificantes. *Materiales de Construcción* 62(307), 359-380. <https://doi.org/10.3989/mc.2012.63610>
- Guan, M., Li, X., Jiang, Z., & Guo, X. (2020). Study on Preparation and properties of low sensitive polycarboxylate superplasticizer. *IOP Conference Series: Materials Science and Engineering* 711(1), 6-11. <https://doi.org/10.1088/1757-899X/711/1/012046>
- Habbaba, A., Lange, A., & Plank, J. (2013). Synthesis and performance of a modified polycarboxylate dispersant for concrete possessing enhanced cement compatibility. *Journal of Applied Polymer Science* 129(1), 346-353. <https://doi.org/10.1002/app.38742>
- Haruehansapong, S., Pulngern, T., & Chucheeesakul, S. (2014). Effect of the particle size of nanosilica on the compressive strength and the optimum replacement content of cement mortar containing nano-SiO<sub>2</sub>. *Construction and Building Materials* 50, 471-477. <https://doi.org/10.1016/j.conbuildmat.2013.10.002>
- Huang, C., & Wang, D. (2017). Surface Modification of nano-SiO<sub>2</sub> particles with polycarboxylate ether-based superplasticizer under microwave irradiation. *ChemistrySelect* 2(29), 9349-9354. <https://doi.org/10.1002/slct.201701493>
- Huynh, K. H., Pham, X. H., Hahm, E., An, J., Kim, H. M., Jo, A., Seong, B., Kim, Y. H., Son, B. S., Kim, J., Rho, W. Y., & Jun, B. H. (2020). Facile histamine detection by surface-enhanced raman scattering using SiO<sub>2</sub>@Au@Ag alloy nanoparticles. *International Journal of Molecular Sciences* 21(11), 1-11. <https://doi.org/10.3390/ijms21114048>
- Jo, B. W., Kim, C. H., Tae, G. ho, & Park, J. Bin. (2007). Characteristics of cement mortar with nano-SiO<sub>2</sub> particles. *Construction and Building Materials* 21(6), 1351-1355. <https://doi.org/10.1016/j.conbuildmat.2005.12.020>
- Khudhair, M. H. R., Elyoubi, M. S., & Elharfi, A. (2018). Study of the influence of water reducing and setting retarder admixtures of polycarboxylate"superplasticizers" on physical and mechanical properties of mortar and concrete. *Journal of Materials and Environmental Science* 9(1), 56-65. <https://doi.org/10.26872/jmes.2018.9.1.7>
- Kooshkaki, A., & Eskandari-Naddaf, H. (2019). Effect of porosity on predicting compressive and flexural strength of cement mortar containing micro and nano-silica by multi-objective ANN modeling. *Construction and Building Materials* 212, 176-191. <https://doi.org/10.1016/j.conbuildmat.2019.03.243>
- Kumar Mehta, P., & Monteiro, P. J. M. (2006). *CONCRETE Microstructure, Properties, and Materials* (McGraw-Hill (ed.); Third). <https://www.ptonline.com/articles/how-to-get-better-mfi-results>
- Lange, A., & Plank, J. (2015). Optimization of comb-shaped polycarboxylate cement dispersants to achieve fast-flowing mortar and concrete. *Journal of Applied Polymer Science* 132(37). <https://doi.org/10.1002/app.42529>
- Lavergne, F., Belhadi, R., Carriat, J., & Ben Fraj, A. (2019). Effect of nano-silica particles on the hydration, the rheology and the strength development of a blended cement paste. *Cement and Concrete Composites* 95, 42-55. <https://doi.org/10.1016/j.cemconcomp.2018.10.007>
- Lei, L., Palacios, M., Plank, J., & Jeknavorian, A. A. (2022). Interaction between polycarboxylate superplasticizers and non-calcined clays and calcined clays: A review. *Cement and Concrete Research* 154(February 2021), 106717. <https://doi.org/10.1016/j.cemconres.2022.106717>
- Lin, X., Pang, H., Wei, D., & Liao, B. (2021). Effects of crosslinked polycarboxylate superplasticizers with crosslinking agent containing ester and amide groups on the properties of cementitious systems. *Journal of Applied Polymer Science* 138(40). <https://doi.org/10.1002/app.51171>
- Lv, S. H., Gao, R. J., & Li, D. (2012). Synthesis of polycarboxylate superplasticizer with  $\beta$ -cyclodextrins as side chain. *Advanced Materials Research* 455-456, 606-611. <https://doi.org/10.4028/www.scientific.net/AMR.455-456.606>
- Ma, X. (2010). Synthesis of new polyether polycarboxylate superplasticizer. *Journal of*

Wuhan University of Technology-Mater. Sci. Ed. 25(5), 799-802. <https://doi.org/10.1007/s11595-010-0095-y>

- Madadi, A. & Wei, J. (2022). Characterization of calcium silicate hydrate gels with different calcium to silica ratios and polymer modifications. *Gels* 8(2), 75. <https://doi.org/10.3390/gels8020075>
- Mohammadpour, R., Yazdimamaghani, M., Reilly, C. A., & Ghandehari, H. (2019). Transient receptor potential ion channel-dependent toxicity of silica nanoparticles and poly(amido amine) dendrimers. *Journal of Pharmacology and Experimental Therapeutics* 370(3), 751-760. <https://doi.org/10.1124/jpet.118.253682>
- Najjigivi, A., Khaloo, A., Iraj Zad, A., & Abdul Rashid, S. (2013). Investigating the effects of using different types of SiO<sub>2</sub> nanoparticles on the mechanical properties of binary blended concrete. *Composites Part B: Engineering* 54(1), 52-58. <https://doi.org/10.1016/j.compositesb.2013.04.035>
- Noaman, A. T., Abed, M. S., & Abdul Hamead, A. A. (2020). Production of polycarboxylate-ether superplasticizer (PCE) coated sand with modified hardened properties in cement mortar. *Construction and Building Materials* 245, 118442. <https://doi.org/10.1016/j.conbuildmat.2020.118442>
- Papatzani, S., & Paine, K. (2018). Polycarboxylate/nanosilica-modified quaternary cement formulations - enhancements and limitations. *Advances in Cement Research* 30(6), 256-269. <https://doi.org/10.1680/jadcr.17.00111>
- Pereira, P., Evangelista, L., & De Brito, J. (2012). The effect of superplasticisers on the workability and compressive strength of concrete made with fine recycled concrete aggregates. *Construction and Building Materials* 28(1), 722-729. <https://doi.org/10.1016/j.conbuildmat.2011.10.050>
- Plank, J., Pöllmann, K., Zouaoui, N., Andres, P. R., & Schaefer, C. (2008). Synthesis and performance of methacrylic ester based polycarboxylate superplasticizers possessing hydroxy terminated poly(ethylene glycol) side chains. *Cement and Concrete Research* 38(10), 1210-1216. <https://doi.org/10.1016/j.cemconres.2008.01.007>
- Plank, Johann, Schroefl, C., Gruber, M., Lesti, M., & Sieber, R. (2009). Effectiveness of polycarboxylate superplasticizers in ultra-high strength concrete: The importance of PCE compatibility with silica fume. *Journal of Advanced Concrete Technology* 7(1), 5-12. <https://doi.org/10.3151/jact.7.5>
- Puerto Suárez, J. D., Uribe C., S. L., Lizarazo-Marriaga, J., & Cárdenas-Pulido, J. (2022). Optimal nanosilica dosage in mortars and concretes subject to mechanical and durability solicitations. *European Journal of Environmental and Civil Engineering* 26(5), 1757-1775. <https://doi.org/10.1080/19648189.2020.1731715>
- Raheem, A. A., Abdulwahab, R., & Kareem, M. A. (2021). Incorporation of metakaolin and nanosilica in blended cement mortar and concrete- A review. *Journal of Cleaner Production* 290, 125852. <https://doi.org/10.1016/j.jclepro.2021.125852>
- Ren, C., Hou, L., Li, J., Lu, Z., & Niu, Y. (2020). Preparation and properties of nanosilica-doped polycarboxylate superplasticizer. *Construction and Building Materials* 252, 119037. <https://doi.org/10.1016/j.conbuildmat.2020.119037>
- Ren, Q., Zou, H., Liang, M., Wang, Y., & Wang, J. (2014). Preparation and characterization of amphoteric polycarboxylate and the hydration mechanism study used in portland cement. *RSC Advances* 4(83), 44018-44025. <https://doi.org/10.1039/c4ra05542j>
- Reyna-Martínez, R., Narro-Céspedes, R.I., Reyes-Acosta, Y.K., Martínez-Luevanos, A., Zugasti-Cruz, A., Neira-Velázquez, M.G., Sánchez-Valdés, S., Soria-Arguello, G., & Ibarra-Alonso, M.C. (2020). Effect of thermal and argon plasma treatment in SiO<sub>2</sub> spheres, assessing the effectiveness in the elimination of organic waste. *Revista Mexicana de Ingeniería Química* 19(3), 1071-1080. <https://doi.org/10.24275/rmiq/Mat906>
- Sathyan, D., Anand, K. B., Mini, K. M., & Aparna, S. (2018). Optimization of superplasticizer in portland pozzolana cement mortar and concrete. *IOP Conference Series: Materials Science and Engineering* 310(1). <https://doi.org/10.1088/1757-899X/310/1/012036>
- Shih, J. Y., Chang, T. P., & Hsiao, T. C. (2006). Effect of nanosilica on characterization of Portland cement composite. *Materials Science and Engineering A* 424(1-2), 266-274. <https://doi.org/10.1016/j.msea.2006.03.010>

- Singh, L. P., Karade, S. R., Bhattacharyya, S. K., Yousuf, M. M., & Ahalawat, S. (2013). Beneficial role of nanosilica in cement based materials - A review. *Construction and Building Materials* 47, 1069-1077. <https://doi.org/10.1016/j.conbuildmat.2013.05.052>
- Stöber, W., Fink, A., & Bohn, E. (1968). Controlled growth of monodisperse silica spheres in the micron size range. *Journal of Colloid and Interface Science* 26(1), 62-69. [https://doi.org/10.1016/0021-9797\(68\)90272-5](https://doi.org/10.1016/0021-9797(68)90272-5)
- Tian, H., Kong, X., Sun, J., Wang, D., & Huang, C. (2019). Fluidizing effects of polymers with various anchoring groups in cement pastes and their sensitivity to environmental temperatures. *Journal of Applied Polymer Science* 136(20), 1-11. <https://doi.org/10.1002/app.47494>
- Vlasenkova, M. I., Dolinina, E. S., & Parfenyuk, E. V. (2019). Preparation of mesoporous silica microparticles by sol-gel/emulsion route for protein release. *Pharmaceutical Development and Technology* 24(2), 243-252. <https://doi.org/10.1080/10837450.2018.1457051>
- Xia, L., Zhou, M., Ni, T., & Liu, Z. (2020). Synthesis and characterization of a novel early-strength polycarboxylate superplasticizer and its performances in cementitious system. *Journal of Applied Polymer Science* 137(30), 1-8. <https://doi.org/10.1002/app.48906>
- Yu, J., Zhang, M., Li, G., Meng, J., & Leung, C. K. Y. (2020). Using nano-silica to improve mechanical and fracture properties of fiber-reinforced high-volume fly ash cement mortar. *Construction and Building Materials* 239, 117853. <https://doi.org/10.1016/j.conbuildmat.2019.117853>
- Zakirov, A. S., Navamathavan, R., Jang, Y. J., Jung, A. S., Lee, K.-M. & Choi, C. K. (2007). Comparative study on the structural and electrical properties of low-k SiOC(-H) films deposited by using plasma enhanced chemical vapor deposition. *Journal of Korean Physical Society* 50(6), 1809. <https://doi.org/10.3938/jkps.50.1809>
- Zhao, H., Liao, B., Nian, F., Zhao, Y., Wang, K., & Pang, H. (2018). Synthesis and characterization of a PAMAM dendrimer-based superplasticizer and its effect on the properties in cementitious system. *Journal of Applied Polymer Science* 135(32), 1-11. <https://doi.org/10.1002/app.46550>
- Zhao, L., Guo, X., Liu, Y., Ge, C., Guo, L., Shu, X., & Liu, J. (2017). Synergistic effects of silica nanoparticles/polycarboxylate superplasticizer modified graphene oxide on mechanical behavior and hydration process of cement composites. *RSC Advances* 7(27), 16688-16702. <https://doi.org/10.1039/C7RA01716B>
- Zhao, Y., Nian, F., Pang, H., Huang, J., Zhao, H., Wang, K., & Liao, B. (2018). Regulating the arm structure of star-shaped polycarboxylate superplasticizers as a means to enhance cement paste workability. *Journal of Applied Polymer Science* 135(21), 1-11. <https://doi.org/10.1002/app.46312>
- Zhu, W., Feng, Q., Luo, Q., Yan, J., & Lu, C. (2022). Investigating the effect of polycarboxylate-ether based superplasticizer on the microstructure of cement paste during the setting process. *Case Studies in Construction Materials* 16(November 2021), e00999. <https://doi.org/10.1016/j.cscm.2022.e00999>
- Zhuang, C., & Chen, Y. (2019). The effect of nano-SiO<sub>2</sub> on concrete properties: A review. *Nanotechnology Reviews* 8(1), 562-572. <https://doi.org/10.1515/ntrev-2019-0050>